PLANT SCIENCE TODAY
Vol x(x): xx–xx
https://doi.org/10.14719/pst.12647

eISSN 2348-1900

RESEARCH ARTICLE

Green synthesis of silver nanoparticles using the methanolic leaves extract of *Bauhinia variegata* L.

Bhawna Kaushal[1], Priyanka Dhiman[1], Alok Kumar Mishra[1] & Rajeev Kumar Gupta[2*]

[1]Department of Microbiology, School of Bioengineering and Biosciences, Lovely Professional University, Phagwara 144 411, Punjab, India
[2]Department of Agronomy, School of Agriculture, Lovely Professional University, Phagwara 144 411, Punjab, India

*Correspondence email - rajeev.30662@lpu.co.in

Received: 09 November 2025; Accepted: 22 March 2026; Available online: Version 1.0: 27 April 2026

Cite this article: Bhawna K, Priyanka D, Alok KM, Rajeev KG. Green synthesis of silver nanoparticles using the methanolic leaves extract of *Bauhinia variegata* L. Plant Science Today (Early Access). https://doi.org/10.14719/pst.12647

Abstract

The synthesis of silver nanoparticles (Ag-NPs) gained significant attention due to their unique physicochemical properties and various applications in biological, environmental and technological disciplines. The biosynthesis of noble metal nanoparticles is a fast-growing research field that is drawing interest from many different scientific areas. In the present study, *Bauhinia variegata* methanol leaf extract was used as a reducing agent and stabiliser during the synthesis of Ag-NPs. The methanol extract of *B. variegata* leaves was analysed by gas chromatography-mass spectrometry (GC-MS). The synthesised silver nanoparticles were characterised by UV-visible spectroscopy, Fourier transform infrared (FTIR), scanning electron microscopy (SEM) and X-ray diffraction techniques. Nanoparticles were characterised using UV-visible spectroscopy and a distinctive absorbance peak at 433 nm was revealed. The zeta potential examination of the produced nanoparticles showed an average zeta potential value of -20.2 mV. The average shape of silver nanoparticles is indicated by SEM (Hitachi S-4500) examination with a diameter of 20–40 nm. The average crystalline size was ~29 nm. This study evaluates green synthesis and traditional methods, highlighting their respective benefits and drawbacks, while also clarifying the essential mechanisms underlying the synthesis of Ag-NPs. The findings suggest that green-synthesised Ag-NPs possess significant potential in medicine and environmental applications.

Keywords: *Bauhinia variegata*; green synthesis; nanotechnology; silver nanoparticles

Introduction

Nanotechnology has gained significant interest in the last few years due to its unique properties, especially the high surface to volume ratio, enhanced surface reactivity, quantum size effect and its use in different fields like medicine, imaging, diagnostics, food packaging, environmental remediation, catalysis and electronics (1). Nanoparticles (NPs) are particles that are between 1 and 100 nm in size. There are 2 kinds of nanoparticles: inorganic and organic nanoparticles. Inorganic nanoparticle includes semiconductor nanoparticles like ZnO, ZnS and CdS; metallic nanoparticles like Au, Ag, Cu and Al; and magnetic nanoparticles like Co, Fe and Ni. In contrast, organic nanoparticles include carbon nanoparticles like fullerenes, quantum dots and carbon nanotubes. Silver nanoparticles are gaining increasing attention due to their unique physicochemical properties and wide range of applications, including medical diagnostics, sensing, imaging, antibacterial therapies and environmental cleanup process (2–4). There are several ways of synthesising different kinds of NPs, like chemical, physical and photochemical methods (5, 6). Silver is a unique material that has been used widely since ancient times. The organisation, size, dispersal and exterior features of silver nanparticles (Ag-NPs) are mostly determined by the amounts of reducing agents, stabilisers and the reaction conditions utilised during the biosynthesis process (7). There are three main ways to make Ag-NPs: chemical, physical and biological. There are two ways to make metallic NPs artificially: from the top down and from the bottom up. The top-down approach involves gradually lithographing or milling larger materials down to the nanoscale. Although this technique works well for producing large quantities of nanoparticles at once, it may not offer much control over their characteristics (8, 9). The bottom-up method, on the other hand, builds nanoparticles from atomic or molecular building blocks, which gives complete control over their size, shape and composition. Some of the methods in this area are chemical vapour deposition and self-assembly (10). Bottom-up methods are harder to use, but they provide more control and are better for industries like electronics and medicine, where it requires specific features of the nanoparticles. The method preferable, will depend on the specific needs of the application and the qualities of the NPs being made. Green synthesis methods have gained attention because they are environmentally friendly and could lead to long-term production (11–14). An eco-friendly approach for making Ag-NPs is highly desirable. This study aims to find a way to make Ag-NPs in an environmentally friendly way using methanol leaves extract (15). The development of green synthesis techniques is driven by growing worries about the environmental implications of standard chemical synthesis methods, which typically use toxic chemicals while producing dangerous byproducts (16, 17). Green synthesis offers an alternative approach by using the ability of different biological resources, such as plant extracts, to reduce and stabilise NPs (18, 19).

The *Bauhinia variegata* L. tree grows in tropical and subtropical areas; it is known for its high phytochemical content, which is a promising option for making Ag-NPs in an environmentally friendly way (20). *Bauhinia variegata* is a member of the family Fabaceae. It is also known as the "camel's foot tree" or the "orchid tree" (21, 22). The plant has been widely used in traditional medicine due to its potential to cure different illnesses (23). Leaves often have more alkaloids, polyphenols and flavonoids, which are bioactive compounds that may have medicinal or therapeutic advantages, which explains why leaves are widely used in medicine compared to other parts like bark or stem (24). These bioactive compounds help to synthesise and keep NPs stable by serving as organic capping and reducing agents. In this study, the extraction process approach uses methanol as a solvent to extract phytochemicals from *B. variegata* leaves. Methanol, a polar solvent, makes it possible to extract a wide spectrum of phytoconstituents, which ensures a thorough representation of the plant's bioactive components (25). The high content of reducing agents in the methanolic leaf extract plays a major role in its ability to act as both a reducing and capping agent in the synthesis of Ag-NPs (26, 27). Silver ions and phytochemicals combine to make stable NPs with their own distinct physical and chemical properties (28). Silver nanoparticles are important due to their antibacterial, anti-inflammatory, anticancer, antioxidative, drug carrier, cosmetics, textiles, antiviral, water treatment and catalytic properties (29, 30). The biosynthesis focuses on using plant-based, renewable materials, which is better for the environment and controls the size and form of nanoparticles very precisely. In addition, *B. variegata* was chosen for its rich phytochemical composition, including flavonoids and phenolics that function as natural reducing and stabilising agents in nanoparticle synthesis. This plant has been recognised for its strong antioxidant, antimicrobial and anti-inflammatory qualities, which make NPs work better, therefore being more effective biologically and better for the environment than other plants. Most of the prior research on *B. variegata* has employed water-based or ethanol-based extracts to make NPs. The present approach uses methanol as it is more polar, which makes it easier to extract a larger range of phytochemicals. It also makes the Ag-NPs more stable and effective at reducing. This methodological innovation differentiates the present study from previous research and offers a novel, environmentally sustainable approach for NP synthesis using *B. variegata*.

Materials and Methods

Collection and extraction of leaves extract

New and healthy *B. variegata* leaves (Fig. 1) were collected in June from Bilaspur, Himachal Pradesh, India, 31.33° N and 76.75° E. Leaves were properly cleaned and washed with water. The sample was retained for shade drying to eliminate the excess water. The *B. variegata* leaves were powdered finely using an electric grinder after being dried in the shade. The extract was then carefully made by mixing 5 g of powdered dried leaves with 100 mL of methanol using the Maceration technique. The previously mentioned composite was then placed in a 48 hr methanol suspension, which enabled the progressive extraction of the various phytochemicals in *B. variegata* leaves. Following the specified suspension time, the mixture was sieved using filter paper made by Whatman No.1. A clean and purified filtrate was produced and the liquid phase was separated from the solid residues using this filtering. The filtrate obtained was carefully preserved in an airtight bottle at 10 °C. After that, it was improved using the different bioactive compounds that were taken from the plant material.

Fig. 1. Fresh leaves of the *Bauhinia variegata* plant, known for their distinctive heart-shaped green leaves.

Phytochemical analysis

The methanol extract of *B. variegata* leaves were analysed by gas chromatography-mass spectrometry (GC-MS). The extraction process was done very carefully to get a wide range of phytochemicals from the plant material. A complicated collection of compounds, each characterised by its own retention time and mass spectrum, was identified by further GC-MS analysis. Helium gas made up 99.999 % of the GC-MS analysis's carrier gas. The AOC -20i + s auto-injector was used to inject 1 µL of the methanol extract from *B. variegata* leaves into the gas chromatograph. The injection port was employed in split-less mode at 250 °C. The GC oven's temperature program started at 50 °C and operated for 5 min. It then rose to 300 °C over the following 2 min at a rate of 2 °C min^{-1}. This temperature was kept for 10 min. The temperature was set at 240 °C for both the ion source and the interface for mass spectrometry. A complete study of the compounds in the methanol extract of *B. variegata* leaves was conducted using a total ion chromatogram across the m/z range of 40–800 (31, 32).

Green synthesis of silver nanoparticles

A combination of 50 mL of a 1 mM solution of silver nitrate ($Ag\text{-}NO_3$) with 5 mL of methanol leaves extract from the *B. variegata* plant was made (Fig. 2). Methanol is effective in extracting polar and slightly nonpolar molecules. This makes silver ions less reactive and more stable. This procedure speeds up the process of making NPs, giving more control over their size and making them more stable. The above procedure was done in the dark to stop photoreduction or alterations caused by light during the production of NPs. During this time, the solution changed hue in a way that was easy to see. This alteration is an essential sign that Ag-NPs are starting to form. The extraction of proteins from plant leaves is due to the reduction process. These proteins help turn silver ions (Ag+) into elemental silver (Ag) by acting as reducing agents.

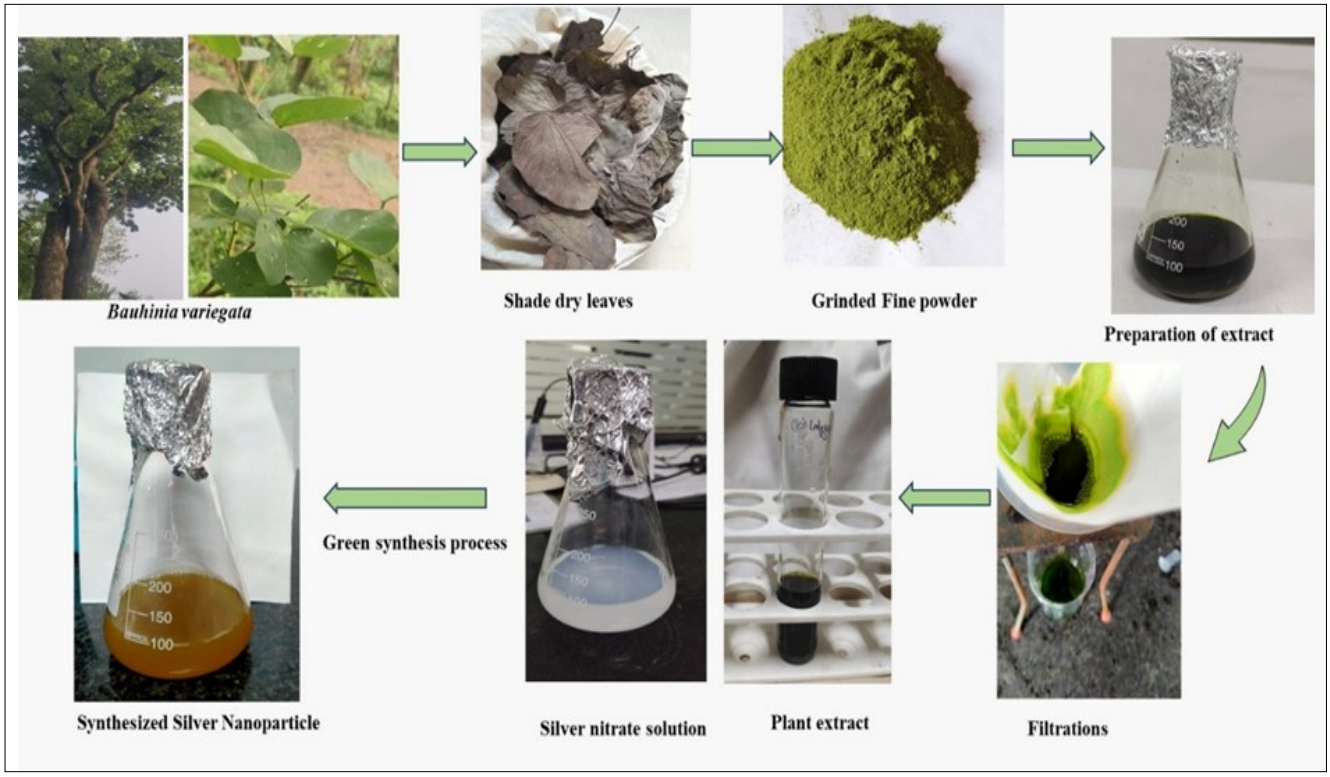

Fig. 2. Green synthesis process.

Characterisation of silver nanoparticles synthesised

A UV-mediated approach using a UV spectrophotometer was used to analyse the Ag-NPs. The research uses UV-visible spectrophotometry to look at the nanoparticles' absorption spectra to learn key aspects like size, shape and concentration. This technology is used to see the synthesis process in real time, which helps to understand how fast the reactions happen. The study not only helps to improve the synthesis settings, but it also serves as a quality control tool to ensure that the UV-mediated synthesis of Ag-NPs is done repeatedly. Fourier transform infrared (FT-IR) spectroscopy was used to determine the sample's infrared spectra. The FT-IR spectra cover the region from 4000 to 450 cm^{-1} with a resolution of 4 cm^{-1}. A potassium bromide (KBr) pellet was manufactured for FT-IR investigation. Potassium bromide is a common sample holder for FT-IR spectroscopy. A small amount of the material is mixed with KBr to create a pellet that allows for the detection of infrared spectra. An X-ray diffractometer was the equipment used to measure X-ray diffraction (XRD). Zeta potential using the Nano-ZS instrument was used to identify the size, shape and structure. The SEM revealed the average size and morphology of the Ag-NPs. Energy dispersive X-ray spectroscopy (EDX) analysis was performed to confirm the presence of elemental silver.

Results and Discussion

Phytochemical analysis

The GC-MS analysis showed that the methanolic extract of *B. variegata* leaves has a lot of bioactive components, with 46 different compounds detected. These bioactive components enhance the complex chemical structure of the plant extract. Retention time (4.026) was seen in the area (0.52) of the discovered chemical 2-(Piperidin-3-yl) ethylamine. Benzyl alcohol was detected at a retention time of 9.275 min with a peak area of 0.78 % and is known to possess antimicrobial properties. The compound 5-hydroxy-4,5-dimethyl-2,5-dihydrofuran-2-one was detected at a retention time of 10.683 min with a peak area of 0.47 %. The compound 4-hydroxy-4-methyl-2-pentanone was detected at a retention time of 10.745 min with a peak area of 2.26 % and is known to possess insecticidal properties. Isobutyl-2-heptenone was detected at a retention time of 14.615 min with a peak area of 0.83 %. The compounds 1,3-dioxane-4-methanol and 4,5-dimethyl-1,3-dioxane were also identified as important constituents. They have concentrations of 0.86 % and retention durations of 16.247 min, respectively. At 17.834 min, 2,4-di-tert-butylphenol was discovered in a lot of 1.52 %, while at 18.667 min, 4-ethenyl-2,6-dimethoxy-phenol was detected in a lot of 0.52 %. At a retention time of 18.806 min, 1-(5-ethyl-tetrahydrofuran-2-yl)-3,3-dimethyl-butan-2-one was detected with a peak area of 0.39 %. This was followed by isopropyl bromoacetate at a retention time of 18.880 min, showing an abundance of 0.80 %. The compound alpha-amino-3′-hydroxy-4′-methoxyacetophenone was identified at 19.015 min with a concentration of 0.47 %. Subsequently, bis(3-oxobutan-2-yl) phthalate was detected at a retention time of 19.060 min with a concentration of 0.52 %. Additionally, the compounds 1-pentadecanol acetate, 2-bromododecane and hexahydropyridine, 1-methyl-4-[4,5-dihydroxyphenyl] were identified at retention times of 19.124, 19.230 and 19.320 min, respectively. At a retention time of 19.365 min, guanosine, 2′-O-methyl- was detected with an abundance of 2.66 %. Followed by, 3-O-Methyl-d-glucose with an abundance of 0.84 % appeared at 19.440 min. 8-Methoxy-2-methyl-6-methylene-7-(trimethylsilyl) methyl-2-undecenethen appeared at 19.495 min with an abundance of 3.25 %. Also detected at 19.562 min was 2-O-Methyl-D-mannopyranose, which had a significant abundance of 3.74 %. With a retention time of 19.655 min and an abundance of 1.27 %, acetic acid, (4,6,8,9-tetramethyl-3-oxabicyclo [3.3.1] non-6-en-1-yl) methyl ester was observed. After 19.780 min, benzophenone with an abundance of 0.44 % and chloromethyl undecanoate with an abundance of 1.28 % were observed. Hexanoic acid, 2-ethyl-3-hydroxy-, methyl ester was identified at a retention time of 20.075

min with an abundance of 5.73 %. A major compound, 4-O-methylmannose, was detected at 20.388 min with a peak area of 38.24 %. At 20.934 min, 1H-indene, 2,3-dihydro-1,1,3-trimethyl-3-phenyl was recorded with an abundance of 0.49 %, followed by adipamide at 21.016 min with a peak area of 0.80 %. After a 0.41 % abundance of tetradecanoic acid, which was detected at 21.467 min, a 0.46 % abundance of 6-Hydroxy-4,4,7a-trimethyl-5,6,7,7a-tetrahydrobenzofuran-2(4H)-one was found at 21.716 min. Additionally, neophytadiene had a retention time of 22.522 min and an abundance of 0.41 %, while 3 Butylindolizidine had a retention time of 21.937 min and an abundance of 0.84 %. Additional compounds detected included 1,2-benzenedicarboxylic acid, bis(2-methylpropyl) ester at a retention time of 22.845 min with an abundance of 0.73 %. At 23.454 min, 7,9 -di-tert-butyl-1-oxaspiro(4,5)deca-6,9-diene-2,8-dione was identified with a higher abundance of 4.56 %. The compound 2β-hydroxy-1β,β-dimethyl was detected at a retention time of 23.515 min with an abundance of 0.49 %. At a retention period of 23.661 min, undecanoic acid, 10-methyl-, methyl ester, was detected with an abundance of 0.76 %. Then, at 24.094 min, n-Hexadecanoic acid was detected at a significant abundance of 5.82 %. The compounds 1,2-Benzenedicarboxylic acid, butyl octyl ester and Benzenepropanoic acid, 3,5-bis(1,1-dimethylethyl)-4-hydroxy-, ethyl ester were detected at 24.274 and 24.524 min, respectively, with an abundance of 1.13 % and 0.46 %, respectively. At 25.623 min, hexanamide, N-pentyl-, was found with an abundance of 0.90 %, while at 25.777 min, 11,14,17-Eicosatrienoic acid, methyl ester, was detected with an abundance of 0.80 %. With an abundance of 0.47 %, [1,1'-Biphenyl]-2,3'-diol, 3,4',5,6'-tetrakis(1,1-dimethylethyl)-was detected at 28.524 min. 1H-Indene, 1-hexadecyl-2,3-dihydro-, another molecule, showed up at 29.989 min with an abundance of 0.45 %. At 30.201 min, 2-hydroxy-1-(hydroxymethyl) ethyl ester, or hexadecanoic acid, was detected with a significant abundance of 1.52 %. In addition, 3,5-Di-tert-butyl-2-hydroxybenzaldehyde, O-pentafluoropropionyl, appears at 34.111 min with an abundance of 0.48 % and alpha. -Tocospiro A emerges at 33.487 min with an abundance of 1.11 %. At 35.930 min, vitamin E was detected with a noteworthy abundance of 4.29 %. Additionally, at 36.961 min, the molecule 3,6,13,16-tetraoxatricyclo [16.2.2.2(8,11)] tetracosa-8,10,18,20,21,23-hexaene-2,7,12,17-tetrone was found with an abundance of 0.54 % (Fig. 3) (Table 1). Several bioactive substances with possible antibacterial, insecticidal and antioxidant qualities were found in the *B. variegata* leaves extract, according to the GC–MS analysis.

Green synthesis of silver nanoparticles

Promising and unique outcomes were obtained from the green production of Ag-NPs utilising methanol leaves extract from *B. variegata*. The reaction mixture was formulated by amalgamating 50 mL of 1 mM $AgNO_3$ solution with 5 mL of the methanolic leaves extract in the dark room at room temperature (~23 °C). The bioactive substances included in the plant extract acted as a catalyst for the reduction of silver ions into NPs, which defined the manufacturing process. Dynamic colour changes seen during the reaction were an important feature of the synthesis. By visual inspection, it was discovered that the *B. variegata* leaves extract quickly took on a yellowish-brown hue after being incubated with an $AgNO_3$ solution (Fig. 4 A). The colour changed to a brown tint after an incubation time of 10 hr (Fig. 4 B). The synthesis process appears to have stabilised or finished when, crucially, no appreciable colour changes were seen during the incubation time. This colour change shows the presence of silver ion reduction and the creation of Ag-NPs. To confirm the biological role of plant metabolites in making NPs, control reactions were done under the same conditions but with a silver nitrate solution without plant extract and denatured methanolic extract. There was no change in the control systems, which shows that the plant extract intact bioactive parts were necessary for this procedure. These metabolites probably worked together as reducing, nucleating and capping agents, which helped the formation of NPs and prevented them from clumping together. In conclusion, the findings show how important *B. variegata* phytochemicals are for creating a simple, long-lasting and effective green synthesis technique for Ag-NPs.

Characterisation of silver nanoparticles synthesised

UV-visible spectrophotometer

The formation of Ag-NPs by the methanolic leaves extract of *B. variegata* was observed using UV–visible spectroscopy. The UV–visible spectral measurements were conducted on a Shimadzu spectrophotometer over 300–600 nm with a resolution of 1 nm. A 1 mL of the reaction mixture was analysed at room temperature and the absorption spectra confirmed the formation of Ag-NPs, displaying a significant peak at 433 nm, suggestive of the surface plasmon resonance of Ag-NPs. The absorbance profile showed the reduction of Ag- ions to Ag^0 NPs, indicating the strong reducing capacity of the phytoconstituents in the *B. variegata* extract. The almost neutral pH (~7.0) of the reaction mixture helped prevent agglomeration and ensured uniform particle dispersion. The identified SPR band signifies that the extract contains chromophoric phytochemicals that serve as reducing and stabilising agents, hence improving the optical properties and stability of the synthesised nanoparticles (Fig. 5).

Fourier transform infrared

To understand the FTIR spectrum of a green synthesis made from *B. variegata* leaves, the unique peaks linked to functional groups in the sample were studied (33, 34). When Ag-NPs are synthesised using procedures that are environmentally friendly, their FTIR spectra display peaks that provide information on the bonding and functional groups within the NPs. The large signal at 3293.84 cm^{-1} suggests that there are hydroxyl groups or water molecules on the surface of the nanoparticle. This is because O-H stretching vibrations are common in phenolic compounds and flavonoids, which confirms their role as reducing agents. Some organic compounds or stabilising agents employed in green synthesis may be the cause of the extremely high wavenumber peak at 2133.69 cm^{-1}, which shows that C<C triple bonds are present. The signal at 1634.69 cm^{-1}, which is associated with C=O stretching vibrations typically found in carbonyl groups of proteins, flavonoids and other secondary metabolites, suggests that carbonyl groups may arise from ketones or aldehydes. This shows that they play a role in the capping and stability of Ag-NPs. The signal at 1016.14 cm^{-1} also shows C-O stretching vibrations, which means that alcohols, ethers, or phenols might be involved in the process. The peaks at 602.99 cm^{-1} and 410.79 cm^{-1} are lower in frequency and show metal-oxygen (M-O) stretching vibrations. They might be caused by the interaction between silver and oxygen, probably because of compounds employed in the green synthesis to capping or stabilising the silver (Fig. 6).

Table 1. Gas chromatography–mass spectrometry analysis of compounds and their biological activity

Sl.No.	Name	R. Time	Area %	Activity
1.	2-(Piperidin-3-yl)ethylamine	4.026	0.52	Anti-inflammatory and potential for drug development
2.	Benzyl alcohol	9.275	0.78	Antibacterial and antifungal
3.	5-Hydroxy-4,5-dimethyl-2,5-dihydrofuran-2	10.683	0.47	Antibacterial
4.	2-Pentanone, 4-hydroxy-4-methyl-	10.745	2.26	Antimicrobial
5.	Isobutyl-2-heptenone	14.615	0.83	Antimicrobial, Cytotoxic
6.	1,3-Dioxane-4-methanol, 4,5-dimethyl-	16.247	0.86	Antibacterial and antifungal
7.	2,4-Di-tert-butylphenol	17.834	1.52	Antioxidant, antibacterial and antifungal
8.	Phenol, 4-ethenyl-2,6-dimethoxy-	18.667	0.52	Antioxidant, antimicrobial, anti-inflammatory
9.	1-(5-Ethyl-tetrahydrofuran-2-yl)-3,3-dimethyl-butan-2-one	18.806	0.39	Antimicrobial, antioxidant,
10.	Isopropyl bromoacetate	18.880	0.80	Antimicrobial and enzyme inhibition
11.	alpha-Amino-3'-hydroxy-4'-methoxyacetophenone	19.015	0.47	No activity found
12.	Bis(3-oxobutan-2-yl) phthalate	19.060	0.52	Antibacterial
13.	1-Pentadecanol acetate	19.124	0.95	Antimicrobial and cytotoxic
14.	2-Bromo dodecane	19.230	2.08	No activity found
15.	Hexahydropyridine, 1-methyl-4-[4,5-dihydroxyphenyl]-	19.320	1.66	Antioxidant, Antimicrobial and anti-inflammatory
16.	Guanosine, 2'-O-methyl-	19.365	2.66	Antiviral, Anticancer and immunomodulatory
17.	3-O-Methyl-d-glucose	19.440	0.84	No activity found
18.	8-Methoxy-2-methyl-6-methylene-7-(trimethylsilyl)methyl-2-undecene	19.495	3.25	No activity found
19.	2-O-Methyl-D-mannopyranosa	19.562	3.74	Antibacterial and anti-inflammatory
20.	Acetic acid, (4,6,8,9-tetramethyl-3-oxabicyclo[3.3.1]non-6-en-1-yl)methyl ester	19.655	1.27	Antimicrobial, anti-inflammatory and cytotoxic
21.	Benzophenone	19.780	0.44	Antimicrobial, antifungal and anti-inflammatory
22.	Chloromethyl undecanoate	19.912	1.28	Anticancer
23.	Hexanoic acid, 2-ethyl-3-hydroxy-, methyl ester	20.075	5.73	Antibacterial
24.	4-O-Methylmannose	20.388	38.24	Antibacterial, anti-inflammatory, antidiabetic and antioxidant
25.	1H-Indene, 2,3-dihydro-1,1,3-trimethyl-3-phenyl-	20.934	0.49	Anticancer
26.	Adipamide	21.016	0.80	Antimicrobial, anti-inflammatory and anticancer
27.	Tetradecanoic acid	21.467	0.41	Antimicrobial
28.	6-Hydroxy-4,4,7a-trimethyl-5,6,7,7a-tetrahydrobenzofuran-2(4H)-one	21.716	0.46	Antimicrobial, anti-inflammatory and cytotoxic
29.	3-Butylindolizidine	21.937	0.84	
30.	Neophytadiene	22.522	0.41	Antimicrobial, anti-inflammatory, analgesic, anticonvulsant and antioxidant
31.	1,2-Benzenedicarboxylic acid, bis(2-methylpropyl) ester	22.845	0.73	Antimicrobial
32.	7,9-Di-tert-butyl-1-oxaspiro[4.5]deca-6,9-diene-2,8-dione	23.454	4.56	No activity found
33.	2.beta.-HYDROXY-1.beta.,(4A).beta.-DIME	23.515	0.49	Anticancer, antimicrobial, anti-inflammatory, antifungal and antibacterial
34.	Undecanoic acid, 10-methyl-, methyl ester	23.661	0.76	Anticancer, antimicrobial and anti-inflammatory
35.	n-Hexadecanoic acid	24.094	5.82	Anti-inflammatory
36.	1,2-Benzenedicarboxylic acid, butyl octyl ester	24.274	1.13	No activity found
37.	Benzenepropanoic acid, 3,5-bis(1,1-dimethylethyl)-4-hydroxy-, methyl ester	24.524	0.46	Antimicrobial and anti-inflammatory
38.	Hexanamide, N-pentyl-	25.623	0.90	Antimicrobial and anti-inflammatory
39.	11,14,17-Eicosatrienoic acid, methyl ester	25.777	0.80	Antibacterial, anti-candidal, anti-inflammatory
40.	[1,1'-Biphenyl]-2,3'-diol, 3,4',5,6'-tetrakis(1,1-dimethylethyl)-	28.524	0.47	Antioxidant, anti-inflammatory and antimicrobial
41.	1H-Indene, 1-hexadecyl-2,3-dihydro-	29.989	0.45	Anticancer, antimicrobial and anti-inflammatory
42.	Hexadecanoic acid, 2-hydroxy-1-(hydroxymethyl)ethyl ester	30.201	1.52	Pesticidal and nematicidal, hypocholesterolemic, 1H-Indene, 1-hexadecyl-2,3-dihydro and antioxidant
43.	.alpha.-Tocospiro A	33.487	1.11	Cytotoxic, antimicrobial, anti-inflammatory and antioxidant
44.	3,5-Di-tert-butyl-2-hydroxybenzaldehyde	34.111	0.48	Antioxidant
45.	Vitamin E	35.930	4.29	Antioxidant
46.	3,6,13,16-Tetraoxatricyclo[16.2.2.2(8,11)]tetracosa-1(20),8,10,18,21,23-hexaene-2,7,12,17-tetrone	36.961	0.54	No activity found

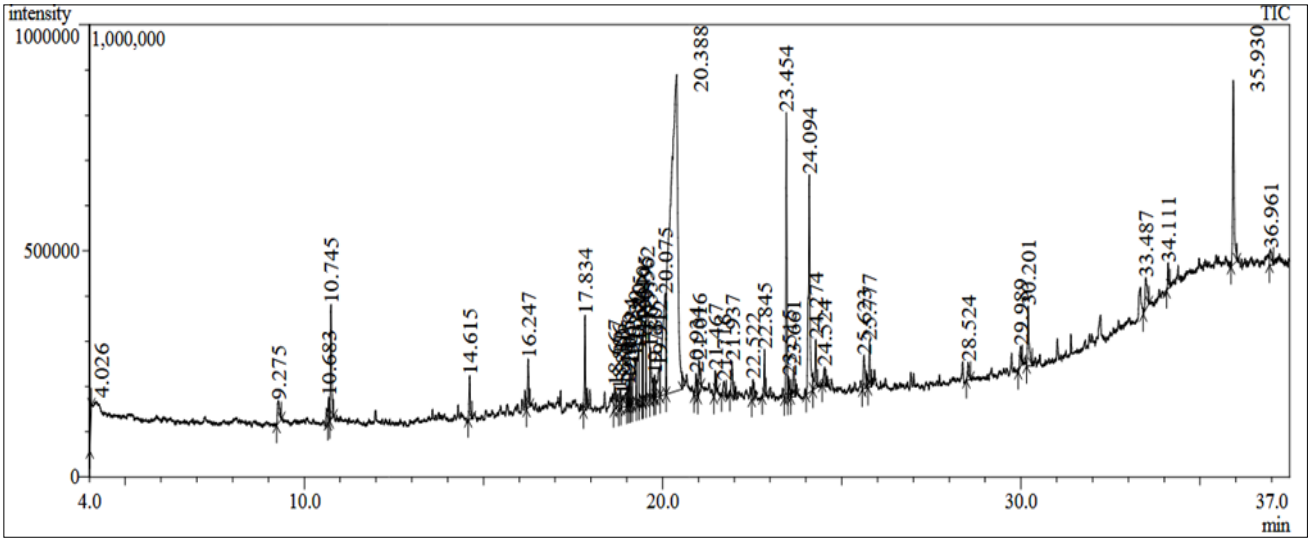

Fig. 3. Gas chromatography–mass spectrometry analysis- 46 bioactive compounds were found in the extract of the *Bauhinia variegata* plant.

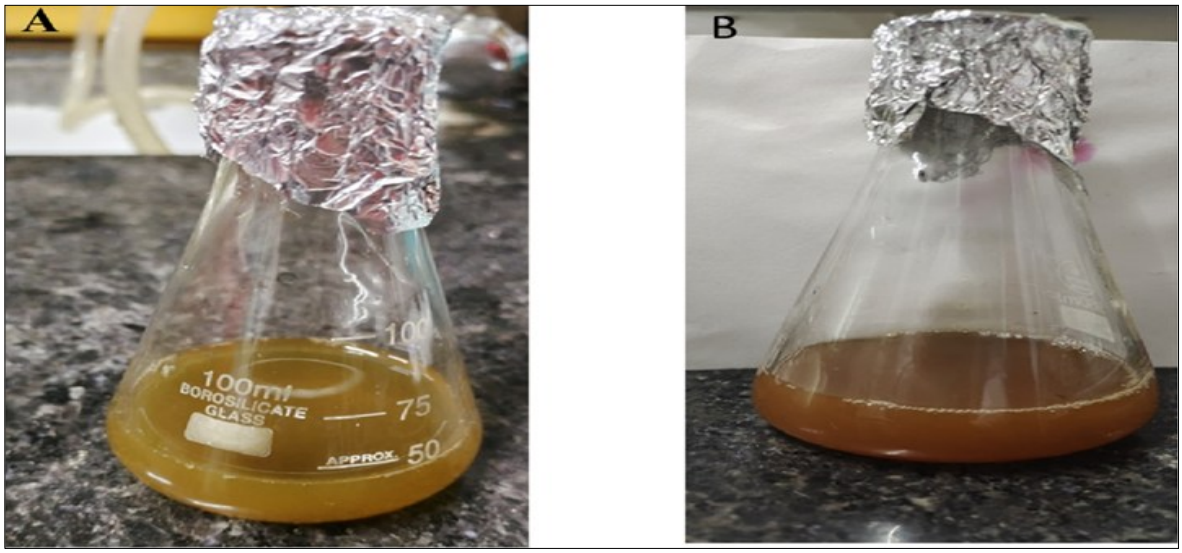

Fig. 4. Colour change of silver nitrate solution after addition of *Bauhinia variegata* methanol extract: (A) Light brown colour after extract addition; (B) Dark brown colour after 10 hr incubation.

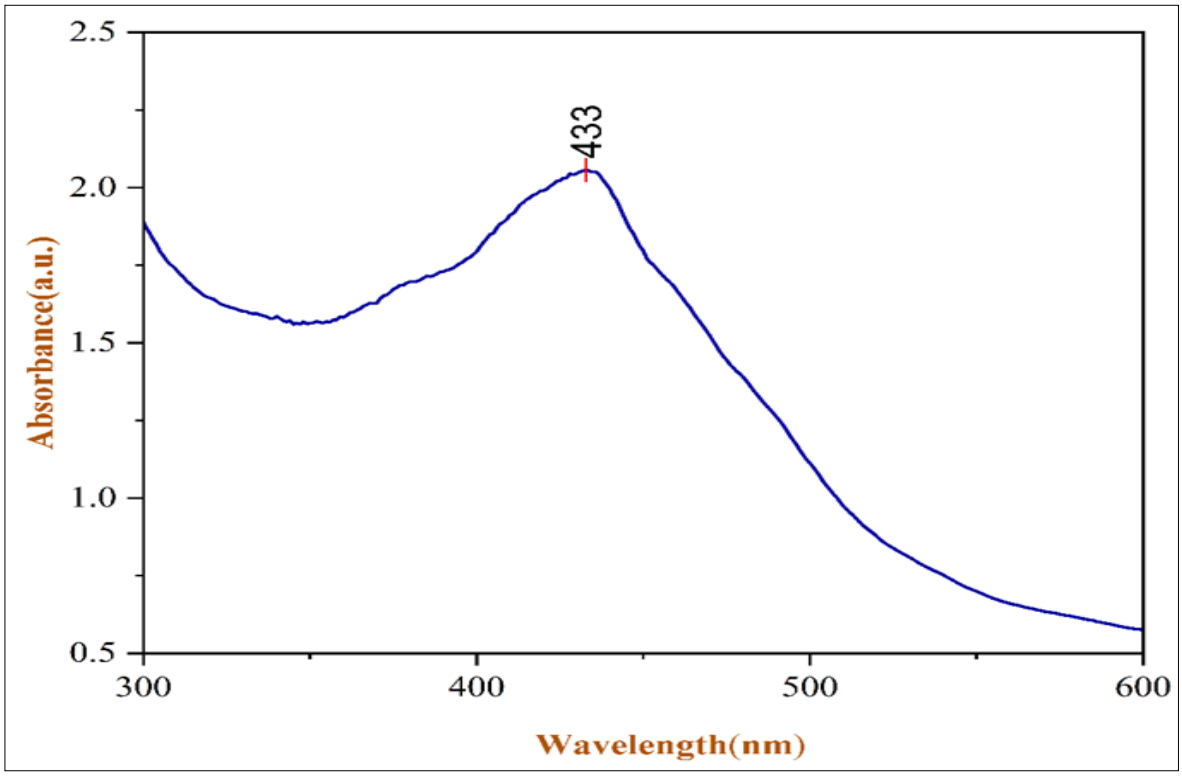

Fig. 5. UV-spectrum of silver nanoparticles synthesised by *Bauhinia variegata* extract.

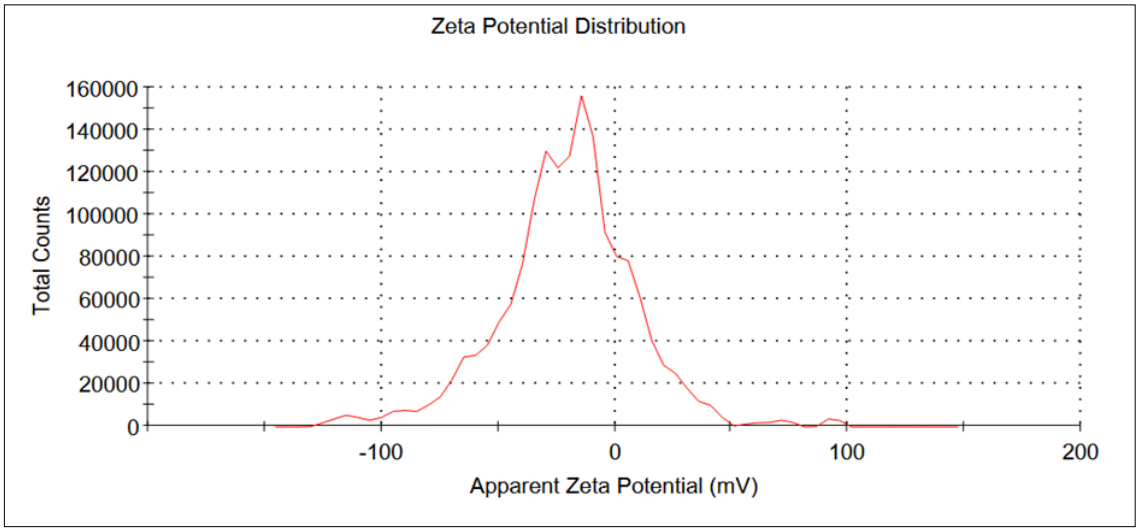

Fig. 6. Zeta potential of silver nanoparticles synthesised by *Bauhinia variegata* extract.

Zeta potential

The zeta potential examination on the NPs indicated that they were stable in a colloidal condition, with an average zeta potential value of -20.2 mV and a zeta deviation of 29.4 mV. The suspension had a conductivity of 0.103 mS/cm, which means it was properly mixed with the medium. The negative surface charge is probably caused by bioactive phytochemicals in the *B. variegata* extract, notably flavonoid and phenolic components. These compounds function as reducing and capping agents, coating the nanoparticles' surfaces and providing electrostatic stability. The zeta potential profile demonstrates that Ag-NPs have been produced that are reasonably stable and well-dispersed. Functional groups from plants help keep these NPs stable (Fig. 7).

X-ray diffraction

This measurement shows that Ag-NPs are made up of crystals. The XRD pattern of the green synthesised silver nanoparticles shows a clear pattern of peaks at 2θ values of about 29.1303, 31.6849, 37.8348, 43.9847, 47.6747, 64.2795 and 77.2416. These peaks match the (100), (100), (110), (110), (111), (200) and (211) planes of the face-centred cubic (FCC) structure of silver. High crystallinity and phase purity are indicated by the peaks' high intensity and sharpness; no discernible imperfections were found (Fig. 8). The XRD used the Scherrer equation for the FCC structure of silver to get the average crystalline size. This showed that the average crystallite size is around 29 nm.

Scanning electron microscopy

The SEM (Hitachi S-4500) measurements provide morphological features and average particle size details of the biological Ag-NPs. The SEM analysis of the green-synthesised Ag-NPs provides essential insights into their structural and morphological characteristics. They are mostly round and spread out, with a diameter range of 20 to 40 nm. The NPs' smooth, even surface implies that they are quite crystalline and that the green manufacturing method worked well. The NPs' low aggregation and good dispersion show that they are stable and can be made quickly (Fig. 9). Energy dispersive X-ray spectroscopy verified the existence of elemental silver in the biosynthesised NPs. The EDX spectra showed big Ag peaks (4.29 wt %) along with carbon (61.5 wt %) and oxygen (33.8 wt %) that came from phytochemicals that worked as reducing and stabilising agents. There was a small amount of chlorine (0.41 wt %) that probably came from leftover plant debris (Fig. 10). The environmentally friendly production of Ag-NPs from *B. variegata* leaves extract is a new application and has not been studied before. The extract's strong ability to reduce and stabilise is what makes the NPs take on a clear structure. The research also shows that the NPs that were made had improved antibacterial properties, which suggests that they might be used in more sophisticated medical

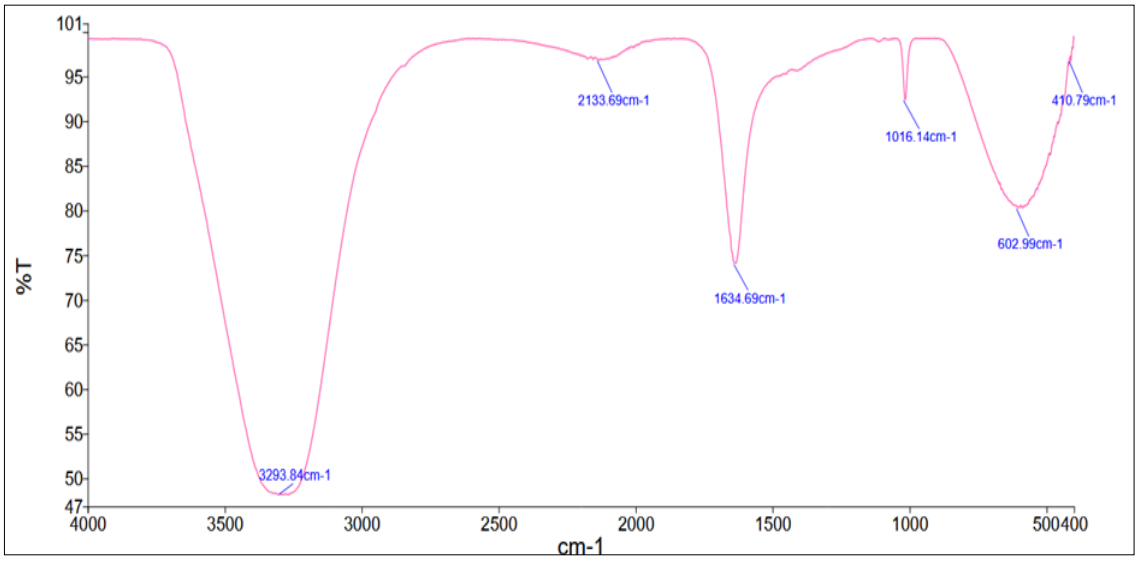

Fig. 7. Fourier transform infrared spectroscopy spectrum of silver nanoparticles synthesised by *Bauhinia variegata* extract.

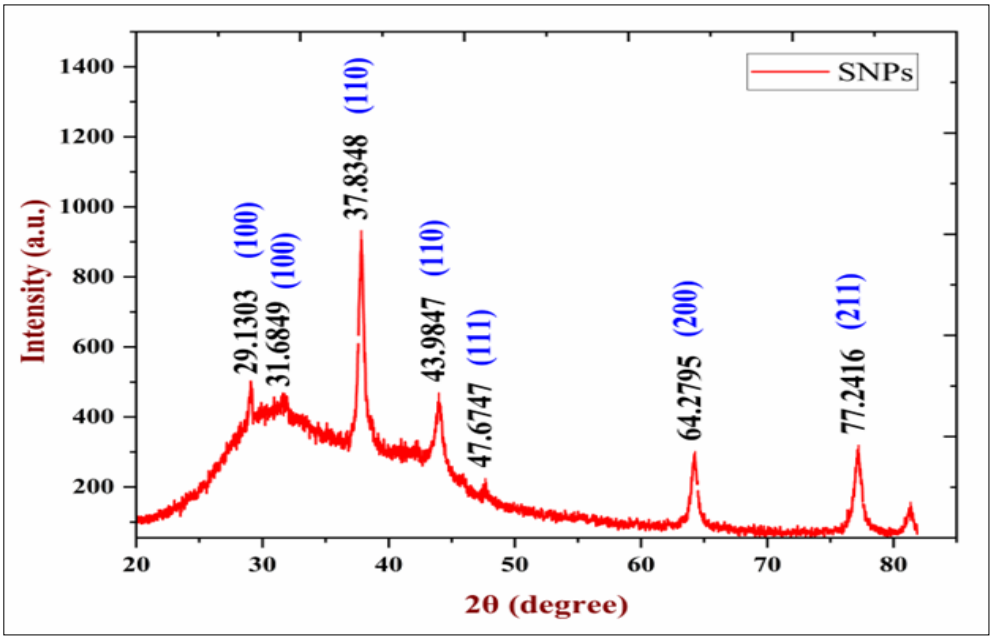

Fig. 8. X-ray diffraction of silver nanoparticles synthesised by *Bauhinia variegata* extract.

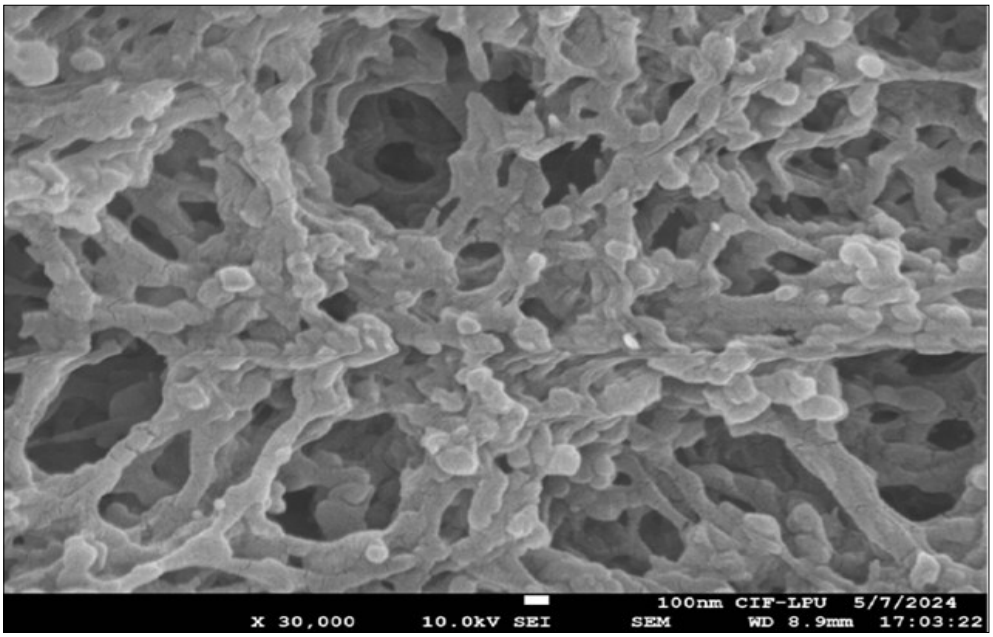

Fig. 9. Scanning electron microscopy of silver nanoparticles synthesised by *Bauhinia variegata* extract.

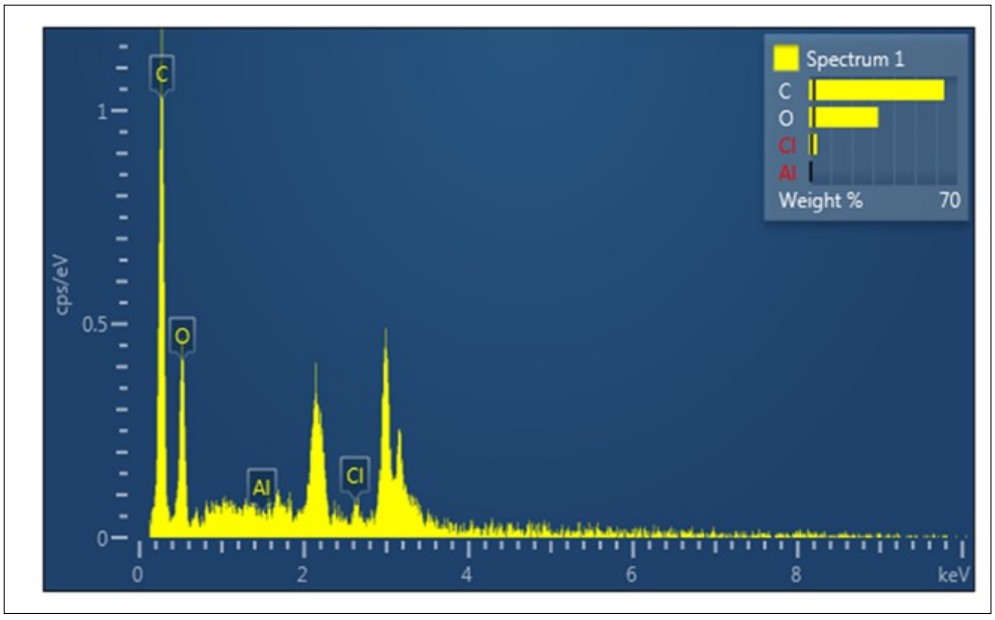

Fig. 10. Energy dispersive X-ray spectroscopy silver nanoparticle synthesised by *Bauhinia variegata* extract.

applications. The study also highlights a more sustainable, environmentally friendly synthesis procedure compared to earlier techniques.

Conclusion

This study efficiently demonstrates the environmentally friendly synthesis of silver nanoparticles utilising the methanolic leaf extract of *Bauhinia variegata* as both a reducing and stabilising agent. This green synthesis process is a long-lasting, safe alternative to typical chemical procedures. The phytochemical portion of *B. variegata* helped Ag^{+} ions turn into Ag^{o}; the nanoparticles were the right size, had a uniform spherical shape and were more stable. The characterisation using GC-MS, UV-Vis, FTIR, zeta-potential, XRD, SEM and EDX validated the synthesis of crystalline, well-dispersed Ag-NPs displaying notable surface plasmon resonance interaction and elemental purity. This study presents the production of Ag-NPs mediated by the methanolic extract of *B. variegata*, highlighting the extract's significant reducing ability and its contribution to the formation of stable nanostructures. It also shows that it is possible to use proteins from plants to make nanomaterials sustainably. This opens new areas of research into how to improve, make large quantities and use environmentally friendly nanoparticles.

Acknowledgements

The authors gratefully acknowledge Lovely Professional University for providing the necessary facilities and continuous support for this research.

Authors' contributions

BK conducted the experiment and wrote the manuscript. PD performed the experimentation. AKM and RKG designed the study and proofread the manuscript. All authors read and approved the final manuscript.

Compliance with ethical standards

Conflict of interest: Authors do not have any conflict of interests to declare.

Ethical issues: None

References

1. Panigrahy M, Rout GR. Nanomaterials in food processing, packaging preservation and their effects on health & environment. Eur Food Res Technol. 2025;251:861–75. https://doi.org/10.1007/s00217-025-04676-3
2. Shahzadi S, Fatima S, Shafiq Z, Janjua MR. A review on green synthesis of silver nanoparticles (SNPs) using plant extracts: A multifaceted approach in photocatalysis, environmental remediation and biomedicine. RSC Adv. 2025;15:3858–903. https://doi.org/10.1039/d4ra07519f
3. Olawade DB, Wada OZ, Fapohunda O, Egbewole BI, Ajisafe O, Ige AO. Nanoparticles for microbial control in water: Mechanisms, applications and ecological implications. Front Nanotechnol. 2024;6:1427843. https://doi.org/10.3389/fnano.2024.1427843
4. Bahraminezhad S, Mehrasbi MR, Homauoni P, Farahmandkia Z. A comparative analysis of the antibacterial effects of green-synthesised silver nanoparticles with chemically synthesised silver nanoparticles. J Hum Environ Health Promot. 2025;11:175–81. https://doi.org/10.61186/jhehp.11.3.175
5. Singh A, Khan A, Jakhmola V, Parashar T, Suyal J, Verma S, et al. Synthesis, characterisation and application of nanoparticles: An exhaustive survey of recent advances and future directions. J Appl Organomet Chem. 2024;4:190–205. https://doi.org/10.48309/JAOC.2024.445790.1170
6. Ranjbar S, Bakhtiari A, Khosravi N, Ashkavandi SJ, Azamian F, Alijaniha M, et al. Silver nanoparticles: Biomedical applications and future perspectives. J Compos Compd. 2024;6(20). https://doi.org/10.61186/jcc.6.3.2
7. Lithi IJ, Nakib KI, Chowdhury AS, Hossain MS. A review on the green synthesis of metal (Ag, Cu and Au) and metal oxide (ZnO, MgO, Co3O4 and TiO2) nanoparticles using plant extracts for developing antimicrobial properties. Nanoscale Adv. 2025;7:2446–73. https://doi.org/10.1039/d5na00037h
8. Ly MT, Dang-Bao T, Nguyen MT, Lam HH, Tran TK, Phan HP. Exploring a surface-capping role of carboxymethyl cellulose for the synthesis of silver nanoparticles via the induction period in a catalytic hydrogenation. J Mol Struct. 2024;1309:138274. https://doi.org/10.1016/j.molstruc.2024.138274
9. Abid N, Khan AM, Shujait S, Chaudhary K, Ikram M, Imran M, et al. Synthesis of nanomaterials using various top-down and bottom-up approaches, influencing factors, advantages and disadvantages: A review. Adv Colloid Interface Sci. 2022;300:102597. https://doi.org/10.1016/j.cis.2021.102597
10. Borah R, Ag KR, Minja AC, Verbruggen SW. A review on self-assembly of colloidal nanoparticles into clusters, patterns and films: Emerging synthesis techniques and applications. Small Methods. 2023;7:2201536. https://doi.org/10.1002/smtd.202201536
11. Singh YR, Selvam A, Lokhande PE, Chakrabarti S. Sustainability: An emerging design criterion in nanoparticles synthesis and applications. In: Bioinspired and Green Synthesis of Nanostructures: A Sustainable Approach. 2023:65–113. https://doi.org/10.1002/9781394174928.ch4
12. Behera S, Mohapatra S, Behera BC, Thatoi H. Recent updates on green synthesis of lignin nanoparticles and their potential applications in modern biotechnology. Crit Rev Biotechnol. 2024;44:774–94. https://doi.org/10.1080/07388551.2023.2229512
13. Al-Dolaimy F, Kzar MH, Hussein UA, Kareem AT, Mizal TL, Omran AA, et al. Green synthesis and characterisation of inorganic nanoparticles with focus on Au nanoparticles for investigation of *E. coli* detection and treatment. J Inorg Organomet Polym Mater. 2024;34:458–84. https://doi.org/10.1007/s10904-023-02844-0
14. Begum SJ, Pratibha S, Rawat JM, Venugopal D, Sahu P, Gowda A, et al. Recent advances in green synthesis, characterisation and applications of bioactive metallic nanoparticles. Pharmaceuticals. 2022;15:455. https://doi.org/10.3390/ph15040455
15. Sharma A, Chandel V, Roy S. Exploring the bioactive properties and diverse uses of *Bauhinia variegata*: A comprehensive review. Discov Plants. 2025;2:86. https://doi.org/10.1007/s44372-025-00167-7
16. Alqahtani AS, Elbeltagi S. Advancing chemistry sustainably: From synthesis to benefits and applications of green synthesis. J Organomet Chem. 2025;1027:123508. https://doi.org/10.1016/j.jorganchem.2025.123508
17. Khosravi A, Zarepour A, Iravani S, Varma RS, Zarrabi A. Sustainable synthesis: Natural processes shaping the nanocircular economy. Environ Sci Nano. 2024;11:688–707. https://doi.org/10.1039/D3EN00973D
18. Zhou S, Qin Y, Lei A, Liu H, Sun Y, Zhang J, et al. The role of green synthesis metal and metal oxide nanoparticles in oral cancer therapy: A review. J Drug Target. 2025;33:853–76. https://doi.org/10.1080/1061186X.2025.2461091

19. Shah DD, Chorawala MR, Mansuri MK, Parekh PS, Singh S, Prajapati BG. Biogenic metallic nanoparticles: From green synthesis to clinical translation. Naunyn Schmiedebergs Arch Pharmacol. 2024;397:8603–31. https://doi.org/10.1007/s00210-024-03236-y

20. Soliman MK, Hashem AH, Al-Askar AA, AbdElgayed G, Salem SS. Green synthesis of silver nanoparticles from *Bauhinia variegata* and their biological applications. Green Process Synth. 2024; 13(1) . https://doi.org/10.1515/gps-2024-0099

21. Choudhary K, Sidhu MC. Comparative palyno-taxonomic studies of three *Bauhinia* species through scanning electron microscope. Vegetos. 2025. https://doi.org/10.1007/s42535-025-01233-x

22. Dip G, Aggarwal P, Kaur S. Morphological, phytochemical, techno-functional characterisation and antimicrobial potential of *Bauhinia variegata* L. flower and bud powder for various food applications. J Food Meas Charact. 2025;19:1992–2006. https://doi.org/10.1007/s11694-025-03095-y

23. Jamal A. Embracing nature's therapeutic potential: Herbal medicine. Int J Multidiscip Sci Arts. 2023;2:117–26. https://doi.org/10.47709/ijmdsa.v2i1.2620

24. Balan T, Yusari Y, Rajendhiran L, Ghazali NAH, Murugesu S, Fatinathan S, et al. A review of antidiabetic activity of *Bauhinia purpurea* plant and its phytochemical constituents. Asian J Med Health Sci. 2023;6:51–65.

25. Sidhu AK, Verma N, Kaushal P. Role of biogenic capping agents in the synthesis of metallic nanoparticles and evaluation of their therapeutic potential. Front Nanotechnol. 2022;3:801620. https://doi.org/10.3389/fnano.2021.801620

26. Dhaka A, Mali SC, Sharma S, Trivedi R. A review on biological synthesis of silver nanoparticles and their potential applications. Results Chem. 2023;6:101108. https://doi.org/10.1016/j.rechem.2023.101108

27. Kamal Y, Khan T, Haq I, Zahra SS, Asim MH, Shahzadi I, et al. Phytochemical and biological attributes of *Bauhinia variegata* L. (Caesalpiniaceae). Braz J Biol. 2022;82:e257990. https://doi.org/10.1590/1519-6984.257990

28. Habeeb Rahuman HB, Dhandapani R, Narayanan S, et al. Medicinal plants mediated the green synthesis of silver nanoparticles and their biomedical applications. IET Nanobiotechnol. 2022;16:115–44. https://doi.org/10.1049/nbt2.12078

29. Husain S, Nandi A, Simnani FZ, Saha U, Ghosh A, Sinha A, et al. Emerging trends in advanced translational applications of silver nanoparticles: A progressing dawn of nanotechnology. J Funct Biomater. 2023;14. https://doi.org/10.3390/jfb14010047

30. Devi K, Chakroborty S, Pal K, Yadav T, Malviya J, Nath N, et al. Green synthetic approaches of silver nanoparticles for sustainable biomedical applications. J Mol Eng Mater. 2023;11:2440002. https://doi.org/10.1142/s2251237324400021

31. More-Adate P, Lokhande KB, Swamy KV, Nagar S, Baheti A. GC-MS profiling of *Bauhinia variegata* major phytoconstituents with computational identification of potential lead inhibitors of SARS-CoV-2 Mpro. Comput Biol Med. 2022;147:105679. https://doi.org/10.1016/j.compbiomed.2022.105679

32. Jena N, Kumar S. Qualitative phytochemical analysis of leaves of *Santalum album* L. Plants Second Metab. 2025;8. https://doi.org/10.5281/zenodo.15486769

33. Rengarajan S, Thangavel N, Sivalingam AM, Lakshmanan G, Selvakumari J, Pandian A. Green synthesis and characterisation of silver nanoparticles with different solvent extracts of *Sesbania grandiflora* (L.) Poiret and assessment of their antibacterial and antioxidant potentials. Biomass Convers Biorefin. 2025;15:26527–43. https://doi.org/10.1007/s13399-023-04696-7

34. Bhattacharjee S, Ghosh C, Sen A, Lala M. Characterisation of *Firmiana colorata* (Roxb.) R. Br. leaf extract and its silver nanoparticles reveal their antioxidative, anti-microbial and anti-inflammatory properties. Int Nano Lett. 2023;13:235–47. https://doi.org/10.1007/s40089-023-00392-6

Additional information

Peer review: Publisher thanks Sectional Editor and the other anonymous reviewers for their contribution to the peer review of this work.

Reprints & permissions information is available at https://horizonepublishing.com/journals/index.php/PST/open_access_policy

Publisher's Note: Horizon e-Publishing Group remains neutral with regard to jurisdictional claims in published maps and institutional affiliations.

Indexing: Plant Science Today, published by Horizon e-Publishing Group, is covered by Scopus, Web of Science, BIOSIS Previews, Clarivate Analytics, NAAS, UGC Care, etc
See https://horizonepublishing.com/journals/index.php/PST/indexing_abstracting

Publisher information: Plant Science Today is published by HORIZON e-Publishing Group with support from Empirion Publishers Private Limited, Thiruvananthapuram, India.